

## Seasonal variations and water chemical control mechanism of water quality in a suburban river near a coal city: a case study in the Xinbian River of Suzhou City, Anhui Province, China

Yuqi Chen<sup>a,b</sup>, Weihua Peng<sup>id a,b,\*</sup>, Manli Lin<sup>a,b,c</sup>, Xinyi Qiu<sup>d</sup>, Jiankui Liu<sup>e</sup>, Jinchen Zhang<sup>b</sup> and Dong Xu<sup>b</sup>

<sup>a</sup> National Engineering Research Center of Coal Mine Water Hazard Controlling, School of Resources and Civil Engineering, Suzhou University, Suzhou 234000, China

<sup>b</sup> Key Laboratory of Mine Water Resource Utilization of Anhui Higher Education Institutes, School of Resources and Civil Engineering, Suzhou University, Suzhou 234000, China

<sup>c</sup> School of Environment Science and Spatial Informatics, China University of Mining and Technology, Xuzhou 221116, China

<sup>d</sup> Exploration Research Institute, Anhui Provincial Bureau of Coal Geology, Hefei 230001, China

<sup>e</sup> Anhui Geological Environment Monitoring Station, Hefei 230001, China

\*Corresponding author. E-mail: whpeng@ahszu.edu.cn

 WP, 0000-0002-1127-1469

### ABSTRACT

To study the seasonal change rules of water quality indicators and water chemical control mechanisms in the nearby city river Xinbian River, in Suzhou City, Anhui Province, China, nine points were selected and periodically sampled for 12 months. Totally 108 water samples were collected, and basic physical–chemical indicators and routine ions (e.g.,  $\text{Ca}^{2+}$ ,  $\text{Mg}^{2+}$ ,  $\text{Na}^+$ ,  $\text{K}^+$ ,  $\text{SO}_4^{2-}$ ,  $\text{Cl}^-$ ,  $\text{F}^-$ ,  $\text{NO}_3^-$ ,  $\text{CO}_3^{2-}$ , and  $\text{HCO}_3^-$ ) were measured. Piper diagram, Gibbs diagram, and ion ratio method were used. The result shows that the seasonal and upstream-to-downstream variations in pH were less varied, whereas the fluctuation in dissolved oxygen was large. Four ions, namely,  $\text{SO}_4^{2-}$ ,  $\text{F}^-$ ,  $\text{Cl}^-$ , and  $\text{Na}^+$  generally first decreased overall and then changed from spring to winter. The maximum contents of  $\text{SO}_4^{2-}$  (406.03 mg/L),  $\text{Cl}^-$  (250.22 mg/L), and  $\text{Na}^+$  (269.99 mg/L) in single water samples appeared at the S9 sampling point (Suzhou control gate) in March 2020. The dominant hydrochemical types in summer were Na–Ca– $\text{HCO}_3$  and Na–Mg– $\text{SO}_4$ , while Na–Mg– $\text{SO}_4$  and Na–Mg– $\text{HCO}_3$  were the main hydrochemical types in the other seasons. The control factors of water chemical composition vary according to the season. However, rock weathering (e.g., silicate dissolution) is the dominant control factor of water chemistry in the studied river section.

**Key words:** Gibbs diagram, Piper diagram, water chemical control mechanism, water quality, Xinbian River

### HIGHLIGHTS

- The annual water quality indicators of a proposed surface water source in a severely water-deficient city were tested.
- The seasonal change characteristics of water quality indicators and their control mechanisms were revealed.
- Both natural and human factors that affect water quality have been comprehensively analyzed.

## 1. INTRODUCTION

Water is an important material resource on which human beings live (Gbadebo 2020; Kormoker *et al.* 2022). However, with the acceleration of population growth, urbanization, and industrialization processes, the problems regarding water resources, mainly manifested as water shortage and water pollution have become increasingly prominent (Schwarzenbach *et al.* 2010; Khan *et al.* 2021). Compared with groundwater, surface water is highly vulnerable to contamination because of natural and anthropogenic sources, especially in water bodies near cities with high population density (Giri & Singh 2014; Prasad *et al.* 2020). Water pollution has become a global problem. With the acceleration of urbanization and industrialization, urban water bodies generally face different degrees of water environmental pollution. In China, up to 80% of the urban rivers are subject to varying degrees of pollution (Qu & Fan 2010). Pollutants mainly include nitrogen, phosphorus, organic compounds, and heavy metals. Water quality evaluation is an important component of water environment quality evaluation. As an effective means of water pollution adjustment, water quality evaluation plays an important role in water resource management. Water quality evaluation aims to evaluate the quality and utilization value

This is an Open Access article distributed under the terms of the Creative Commons Attribution Licence (CC BY 4.0), which permits copying, adaptation and redistribution, provided the original work is properly cited (<http://creativecommons.org/licenses/by/4.0/>).

of water bodies. Specifically, the water environment quality evaluation is performed according to certain evaluation standards, the selection of relevant water quality parameters, and the use of specific calculation methods. The quality of the water environment is used for scientific evaluation.

Suzhou City, in Anhui Province, is located in the semi-humid area of the Huanghuai region and epitomizes the rapid urbanization and modern agricultural cities in China (Jiang *et al.* 2020). Suzhou City is located in the central part of the Huaibei Plain, with significant differences in geomorphic elements, which can be generally divided into three types: hills, plateaus, and plains. Suzhou City also has abundant coal resources. The Twohuai Base (including Huaibei and Huainan mining areas), where Suzhou is located, is one of the 13 large coal bases in China. The proven coal reserves in Suzhou are  $60 \times 10^8$  t, accounting for more than 75% of the Huaibei coal reserves (Lin *et al.* 2017). At present, groundwater is the only drinking water source in Suzhou City. The water shortage phenomenon is increasingly exposed due to the long-term use of groundwater, groundwater settlement, and the formation of underground tunnels in this area. Previous studies on the Xinbian River have mainly focused on water chemical characteristics (Lin *et al.* 2022), water quality evaluation (Jiang *et al.* 2020; Jiang *et al.* 2021b), hydrological process (Chen *et al.* 2020), health risk assessment (Yu *et al.* 2022), ecological risk assessment (Jiang *et al.* 2021a), and source apportionment of pollutants (Chen *et al.* 2023). For example, Yu *et al.* (2020b) evaluated the water quality status of the Xinbian River by measuring the total nitrogen, total phosphorus, chemical oxygen demand, ammonia nitrogen, and chlorophyll a. Li (2003) comprehensively analyzed the historical water quality data from 1980 to 2000 on the ammonia nitrogen; nitrite nitrogen; and oxygen consumption in the Qilijing, Liuzha, Sixian Bianhe Bridge flow section of the Xinbian River pollution. Yu & Feng (2018) used the ground accumulation index method and the comprehensive index method to evaluate the degree of pollution and the distribution characteristics of heavy metals in the Xinbian River sediment. From the current research progress, considerable studies focus on single survey studies, whereas long-term monitoring and seasonal assessments are rare. Although our previously research had been conducted on health risks (Yu *et al.* 2022), ecological risks (Jiang *et al.* 2021a), and source apportionment (Chen *et al.* 2023) of typical pollutants in the Xinbian River, the seasonal variations and water chemical control mechanism of water quality in the Xinbian River had not yet been studied.

At present, relevant departments plan to build a fourth water plant to alleviate the shortage of water resources. This water plant plans to use the North Huaihe River Diversion Project and the Xinbian River water as its water sources, and its water intake head is located near the reach of the study object. Considering the seasonal variation in surface water quality is crucial in assessing natural or human contributions to river pollution (Giri & Singh 2014); therefore, through a year of continuous sampling monitoring, the focus should be dedicated to studying the water quality index seasonal change law and water chemical control mechanism in the Suzhou Xinbian River. The specific goals of this study were: (1) to investigate the seasonal variation of basic physicochemical indicators and routine ions in Xinbian River; (2) to determine if there are differences in the hydrochemical formation mechanism among different seasons; and (3) to further explore the water chemical control mechanism of Xinbian River. This research is significant for the environmental protection of the Xinbian River and management work.

## 2. MATERIALS AND METHODS

### 2.1. Sampling area

Suzhou is located in the northern part of Anhui Province, between east longitude  $116^{\circ}09'$ – $118^{\circ}10'$  and north latitude  $33^{\circ}18'$ – $34^{\circ}38'$  (Figure 1(b)). The Xinbian River is located in the Huaibei Plain and the north bank of the Huaihe River, running across the provinces of Anhui and Jiangsu. It is a contemporary artificial river located in Suzhou City in Anhui Province (Figure 1(c)) and Sihong County in Suqian City in Jiangsu Province. It belongs to the Hongze Lake water system in the Huaihe River Basin. The construction of the Xinbian River, which mainly aims at solving the external flood and waterlogging disaster and considering agricultural irrigation and shipping development, began in October 1966 and was completed in 1970. Suzhou surface water system is relatively developed. Many rivers exist in the region, and the largest is the Xinbian River, followed by the Tuo River (Chen *et al.* 2020). The Xinbian River is 127.2 km long, starting from Qilingzi in the northwest of Suzhou City, Anhui Province in the west; passes through Lingbi County, Sixian County, and Sihong County in Jiangsu Province; and finally injects into Lihewa at the west end of the Hongze Lake in the west edge of Hongze Lake (Wang 2020). The Xinbian River provides water for irrigation, shipping, water supply, and aquaculture along the river and improves the ecological environment. The water sampling points in this study are shown in Figure 1(d). For

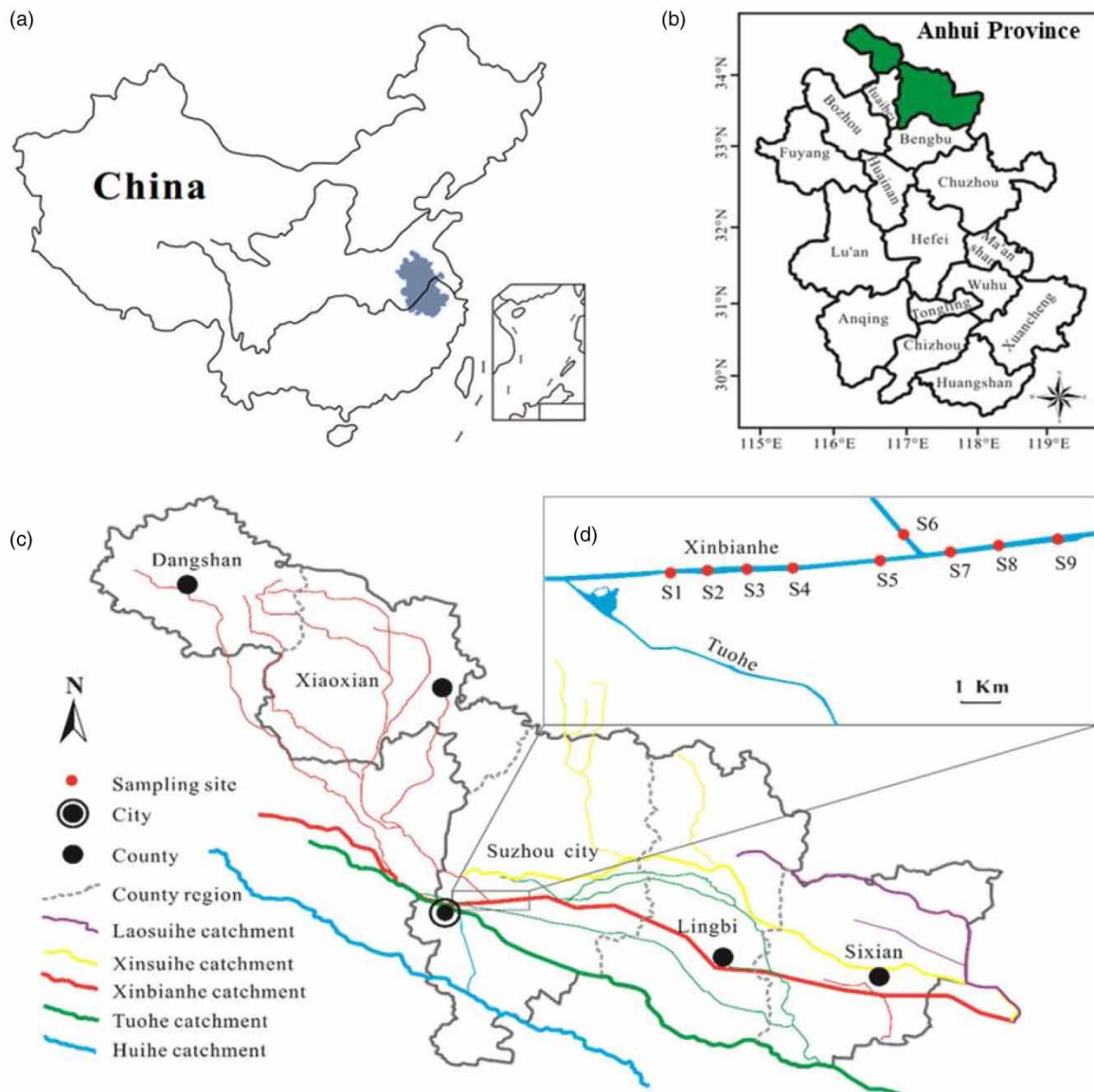


**Figure 1** | Location of the study area and sampling sites. (a) was referenced from Lin *et al.* (2017); (b) was referenced from Chen *et al.* (2020).

the same water sample in the river section, we had previously studied health risks (Yu *et al.* 2022), ecological risks (Jiang *et al.* 2021a), and source apportionment (Chen *et al.* 2023). This study focuses on analyzing the water chemical control mechanism in different seasons.

## 2.2. Sample collection and analysis

### 2.2.1. Sample collection

Considering the location of the proposed surface water plant, the distribution of the main and tributaries of the Xinbian River, as well as the convenience of sampling work, nine sampling site sections (Figure 1(d)) were set up in the Xinbian River (Huaihai North Road to control sluice section). The location of the sampling sites is listed in Table 1. A total of 108 water samples were collected in the middle 10 days of each month from December 2019 to November 2020. The process of sample collection, storage, and transportation, strictly followed the *Technical Specifications Requirements for Monitoring of Surface Water and Waste Water* (HJ/T 91-2002). The sampling containers are polyethylene plastic bottles that have been cleaned with distilled water in advance and then washed thrice at the sampling site. For sampling, a self-made two-way scalable surface water sampler, with a sampling depth of 50 cm below the water surface and a sampling volume of 500 mL/sample, was used.

**Table 1** | Location of sampling sites

Sampling points	Longitude	Latitude	Distance from the surface water plant
S1	116°58'31"	33°40'13"	Upstream ~4,500 m
S2	116°59'2"	33°40'14"	Upstream ~3,500 m
S3	116°59'29"	33°40'15"	Upstream ~3,000 m
S4	116°59'52"	33°40'16"	Upstream ~2,500 m
S5	117°1'45"	33°40'24"	Upstream ~500 m
S6	117°2'19"	33°40'42"	Tributary (Yinhe) ~1,500 m
S7	117°2'38"	33°40'33"	Downstream ~2,000m
S8	117°3'39"	33°40'40"	Downstream ~3,500 m
S9	117°4'45"	33°40'44"	Downstream ~5,000 m

### 2.2.2. Test and analysis of sample indexes

*In situ* sampling: temperature (T); pH; dissolved oxygen (DO); total dissolved solids (TDS); conductivity (Cond); redox potential (ORP), including T, pH, TDS, ORP, Cond by portable test pen (OHAUS, Suite 310); and DO by professional portable DO meter (Wiggens, DO80).

The water samples were sent to the laboratory within 24 h and filtered by a disposable syringe and 0.45 µm microporous filter to a 10 mL centrifugal tube for routine ion testing, including  $\text{Ca}^{2+}$ ,  $\text{Mg}^{2+}$ ,  $\text{Na}^+$ ,  $\text{K}^+$ ,  $\text{SO}_4^{2-}$ ,  $\text{Cl}^-$ ,  $\text{CO}_3^{2-}$ ,  $\text{HCO}_3^-$ ,  $\text{F}^-$ , and  $\text{NO}_3^-$ .

$\text{Ca}^{2+}$ ,  $\text{Mg}^{2+}$ ,  $\text{Na}^+$ ,  $\text{K}^+$ ,  $\text{SO}_4^{2-}$ ,  $\text{Cl}^-$ ,  $\text{F}^-$ , and  $\text{NO}_3^-$  were determined by Thermo Fisher Scientific ICS-900 (ICS-900); whereas  $\text{CO}_3^{2-}$  and  $\text{HCO}_3^-$  were determined by acid-base titration (The balance of sites is controlled within 5%).

### 2.3. Spatiotemporal analysis of water quality indicators

Taking Class III of the *Environmental Quality Standards for Surface Water* (GB 3838-2002) (EPAC & GAQSIQC 2002), the standard limit of the *Standards for Drinking Water Quality* (GB 5749-2022) (SAMRC & SAC 2022), and *Guidelines for Drinking-water Quality* of World Health Organization (WHO 2017) as references, the spatio-temporal variation in the basic physicochemical indexes (e.g., pH, DO, ORP, Cond, TDS, T) and conventional ions (e.g.,  $\text{Ca}^{2+}$ ,  $\text{Mg}^{2+}$ ,  $\text{Na}^+$ ,  $\text{K}^+$ ,  $\text{SO}_4^{2-}$ ,  $\text{Cl}^-$ ,  $\text{F}^-$ ,  $\text{NO}_3^-$ ,  $\text{CO}_3^{2-}$ , and  $\text{HCO}_3^-$ ) were mainly analyzed via bar charts.

### 2.4. Research methods of water chemical mechanism

Using the water chemistry software AqQA (version 1. 5), the main anion and cation compositions of the water sample were analyzed by comparing the Piper triple graph in different seasons of the Xinbian River, and the specific water chemistry type was calculated. The hydrochemical control mechanism (aqueous rock interaction) of the water samples is discussed by using the Gibbs diagram method and ion ratio method. The ion concentration formula of Gibbs is calculated as: Gibbs I =  $\text{Cl}^- / (\text{Cl}^- + \text{HCO}_3^-)$  and Gibbs II =  $(\text{Na}^+ + \text{K}^+) / (\text{Na}^+ + \text{K}^+ + \text{Ca}^{2+})$  (in meq/L). The calculated ion ratio mainly included  $(\text{Mg}^{2+}/\text{Na}^+) / (\text{Ca}^{2+}/\text{Na}^+)$  and  $(\text{HCO}_3^-/\text{Na}^+) / (\text{Ca}^{2+}/\text{Na}^+)$  (in meq/L).

### 2.5. Data processing

Microsoft Excel 2010 and IBM SPSS Statistics 22. 0 were used to perform data processing and statistical analysis, respectively. OriginPro 8 was used to draw the bar charts. Water chemistry software AqQA (version 1. 5) was used to draw Piper diagrams. OriginPro 8 and CorelDRAW2020 were used to draw Gibbs diagrams and ion ratio diagrams.

## 3. RESULTS AND DISCUSSION

### 3.1. Test results and change rules of the basic physicochemical indicators

#### 3.1.1. Statistical analysis of the test results of the basic physicochemical indicators

The test results of the basic physicochemical indicators are listed in Table 2. Among them, except for pH and DO, nearly all the other indicators reached the relevant standard limits of GB 3838-2002 Class III water and GB 5749-2022.

**Table 2** | Test results and comparison of basic physicochemical indexes in Xinbian River ( $n = 108$ )

Index	Range	Mean value	Standard deviation (SD)	CV (%)	GB 3838-2002 <sup>a</sup>	GB 5749-2022 <sup>b</sup>
pH	7.75–9.50	8.6	0.26	2.9	6~9	6.5–8.5
DO (mg/L)	4.71–17.45	8.46	1.92	22.71	$\geq 5$	– <sup>c</sup>
ORP (Mv)	50.00–178.50	118.9	28.79	24.22	–	–
Cond ( $\mu\text{s}$ )	709.0–1,936.5	1,215.23	246.29	20.27	–	–
TDS (mg/L)	196.0–923.0	512.72	182.55	35.60	–	1,000
$T$ ( $^{\circ}\text{C}$ )	7.98–30.53	19.82	7.65	38.62	–	–

<sup>a</sup>Class III water quality standard of Environment Quality Standards for Surface Water (GB 3838-2002).

<sup>b</sup>Standards for Drinking Water Quality (GB 5749-2022).

<sup>c</sup>Not explicitly required.

Out of the 108 water samples tested, 6 had a pH over 9 (5.56%), and 77 exceeded 8.5 (71.30%), with a pH range of 7.75–9.50, a mean of  $8.60 \pm 0.26$ , overall alkalinity, and small dispersion (coefficient of variation (CV) = 2.98%). The number of samples with DO below 5 mg/L is 1 (0.93%).

In view of the basic physicochemical indicators, only pH and DO exceeded the standard. Thus, their seasonal change laws are studied.

### 3.1.2. Seasonal change in pH and DO

The results of the pH and DO tests are shown in Figure 2(a) and 2(b), respectively. The pH showed no obvious differences in seasonal changes; DO increased overall, and its mean values in spring, summer, autumn, and winter were  $7.55 \pm 1.56$ ,  $8.41 \pm 1.27$ ,  $7.92 \pm 1.66$ , and  $9.94 \pm 2.16$  mg/L, respectively. DO is relatively high in winter and relatively low in other seasons, which are mainly related to comprehensive factors, such as temperature, atmospheric reoxygenation, and oxygen consumption of aquatic organisms. Suzhou belongs to the semi-humid monsoon climate of the warm temperate zone of North China, and the Xinbian River rarely freezes during winter. On the one hand, high pressure, high wind speed, and low temperature in winter are conducive to atmospheric reoxygenation; on the other hand, aquatic organisms consume relatively less oxygen during winter, thereby making the DO relatively high during this season (Zhou *et al.* 2020; Zhang *et al.* 2022).

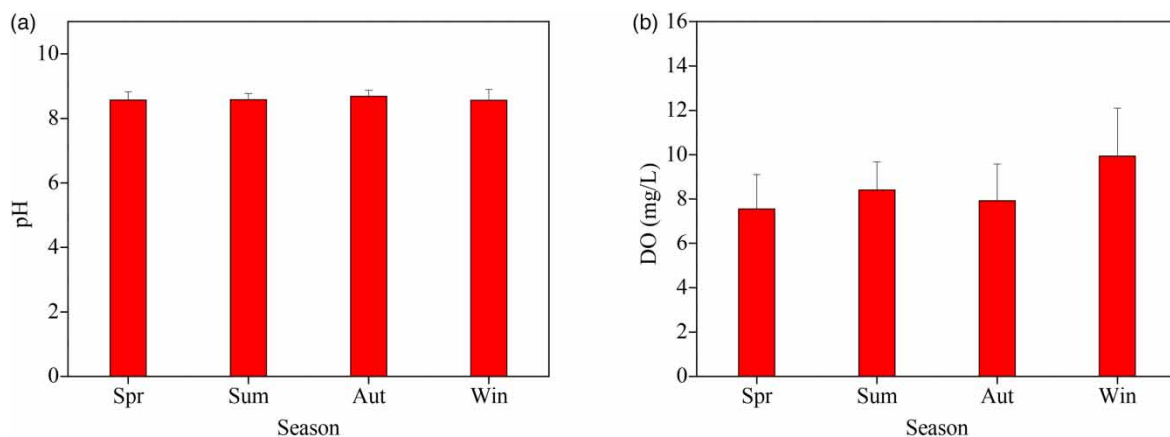


**Figure 2** | Changes in pH and DO over time (by season).

### 3.1.3. Spatial variations in pH and DO

Along the upstream to the downstream direction of the river ( $S1 \rightarrow S9$ ), the changes in pH and DO are shown in Figure 3(a) and 3(b), respectively.

Overall, no significant change is observed along the pH route, whereas the DO route shows an increase first ( $S1 \rightarrow S5$ ) before a decrease ( $S6 \rightarrow S9$ ), in which  $S1 \rightarrow S4$  (Huaihai North Road ~ underground culvert) is generally stable, and the tributary that leads the river into the upstream  $S5$  sampling point ( $9.10 \pm 1.48$  mg/L) and the  $S6$  sampling point ( $8.02 \pm 1.38$  mg/L) has the highest and lowest DO contents. After flowing into the main river

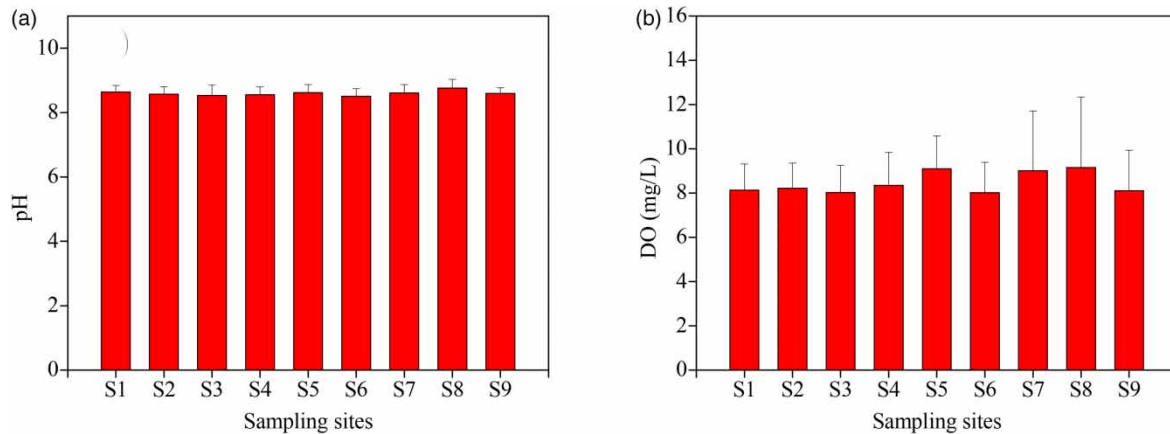


**Figure 3** | Spatial variation in pH and DO along the path.

channel (S6, S9), the DO first increases and then decreases, and the change range is relatively large, which is mainly related to the inflow of the tributary diversion river and the control of water blocking in the sluice.

### 3.2. Test results and change rules of routine ion analysis

#### 3.2.1. Statistical analysis of routine ion test results

Test results of the conventional ion index of the Xinbian River in a whole year ( $\text{Ca}^{2+}$ ,  $\text{Mg}^{2+}$ ,  $\text{Na}^+$ ,  $\text{K}^+$ ,  $\text{SO}_4^{2-}$ ,  $\text{Cl}^-$ ,  $\text{F}^-$ ,  $\text{NO}_3^-$ ,  $\text{CO}_3^{2-}$ , and  $\text{HCO}_3^-$ ) are listed in Table 3. Among the measured ions, nearly all indicators reached the relevant standard limits of GB 3838-2002 and GB5749-2022, except for  $\text{SO}_4^{2-}$ ,  $\text{F}^-$ ,  $\text{Cl}^-$ , and  $\text{Na}^+$ .

**Table 3** | Conventional ion test results and comparison of the Xinbian River ( $n = 180$ )

Index	Content range (mg/L)	Mean value (mg/L)	SD (mg/L)	CV (%)	GB 3838-2002 <sup>a</sup>	GB 5749-2022 <sup>b</sup>	WHO <sup>c</sup>
$\text{Ca}^{2+}$	25.08–69.74	49.50	9.39	18.98	– <sup>d</sup>	–	–
$\text{Mg}^{2+}$	21.18–62.31	41.44	9.77	23.57	–	–	–
$\text{Na}^+$	54.93–269.99	140.00	40.35	28.82	–	200	200
$\text{K}^+$	7.34–14.61	10.85	1.56	14.41	–	–	–
$\text{SO}_4^{2-}$	81.42–406.03	216.15	83.51	38.63	250	250	250
$\text{Cl}^-$	56.76–250.22	138.98	42.92	30.88	250	250	250
$\text{F}^-$	0.53–1.21	0.87	0.18	21.04	1.0	1.0	1.5
$\text{NO}_3^-$	0.00–9.02	2.67	2.52	94.40	10	10	50
$\text{CO}_3^{2-}$	0.00–63.37	3.40	11.06	325.84	–	–	–
$\text{HCO}_3^-$	138.96–360.00	262.82	45.03	17.13	–	–	–

<sup>a</sup>Environment Quality Standards for Surface Water (GB 3838-2002),  $\text{F}^-$  is the limit of Class III water,  $\text{SO}_4^{2-}$ ,  $\text{Cl}^-$ , and  $\text{NO}_3^-$  are the supplementary item standard limits of centralized drinking water surface water sources.

<sup>b</sup>Standards for Drinking Water Quality (GB 5749-2022).

<sup>c</sup>The World Health Organization (WHO) drinking water limit.

<sup>d</sup>No clear requirements.

$\text{SO}_4^{2-}$  ranges from 81.42 to 406.03 mg/L, has a mean of  $216.15 \pm 83.51$  mg/L, and has high dispersion variation ( $\text{CV} = 38.63\% > 36\%$ ). Out of the 108 water samples tested, 39 water samples exceeded the GB 3838-2002 (III) and GB 5749-2022 standard limits (250 mg/L), accounting for 36.11%.

$\text{F}^-$  ranges from 0.53 to 1.21 mg/L, has a mean of  $0.87 \pm 0.18$  mg/L, and has moderate variation in the degree of dispersion ( $\text{CV} = 21.04\%$ , between 16 and 35%). Among the 108 water samples tested, 32 of the water samples exceeded the GB 3838-2002 and GB 5749-2022 standard limits (1.0 mg/L), accounting for 29.63%. However, the content of fluoride in the water samples was lower than the water quality standards (1.5 mg/L) of the World Health Organization (WHO 2017).

The  $\text{Cl}^-$  ranges from 56.76 to 250.22 mg/L, has a mean of  $138.98 \pm 42.92$  mg/L, and has moderate variation in the degree of dispersion ( $\text{CV} = 30.88\%$ , between 16 and 35%). Among the 108 water samples tested, only one slightly exceeded the GB 3838-2002 and GB 5749-2022 standard limits (250 mg/L), accounting for 0.93%.

GB 3838-2002 has no clear requirement for  $\text{Na}^+$ , whereas GB 5749-2022 requires  $\text{Na}^+$  as an unconventional indicator with a limit value of 200 mg/L. In this study,  $\text{Na}^+$  ranged from 54.93 to 269.99 mg/L, has a mean of  $140.00 \pm 40.35$  mg/L, and has moderate variation in the dispersion degree ( $\text{CV} = 28.82$ , between 16 and 35%). Among the 108 water samples tested, 9 water samples exceeded the GB 5749-2022 standard limit (200 mg/L), accounting for 8.33%.

Other ions do not exceed the standard, so we focused on the seasonal and spatial variations of these four ions.

### 3.2.2. Seasonal changes in main ions

The results of the four ion tests, namely,  $\text{SO}_4^{2-}$ ,  $\text{F}^-$ ,  $\text{Cl}^-$ , and  $\text{Na}^+$ , are shown in Figure 4. All four ions showed a trend of decreasing and then increasing with the season, and the maximum seasonal means of  $\text{SO}_4^{2-}$ ,  $\text{F}^-$ ,  $\text{Cl}^-$ , and  $\text{Na}^+$  appeared in spring, with  $313.64 \pm 49.49$ ,  $1.06 \pm 0.08$ ,  $189.76 \pm 23.71$ , and  $174.77 \pm 28.79$  mg/L, respectively; while the minimum seasonal mean values of the four ions appeared in autumn with contents of  $144.08 \pm 21.82$ ,  $0.69 \pm 0.059$ ,  $96.65 \pm 3.91$ , and  $106.58 \pm 8.19$  mg/L, respectively.

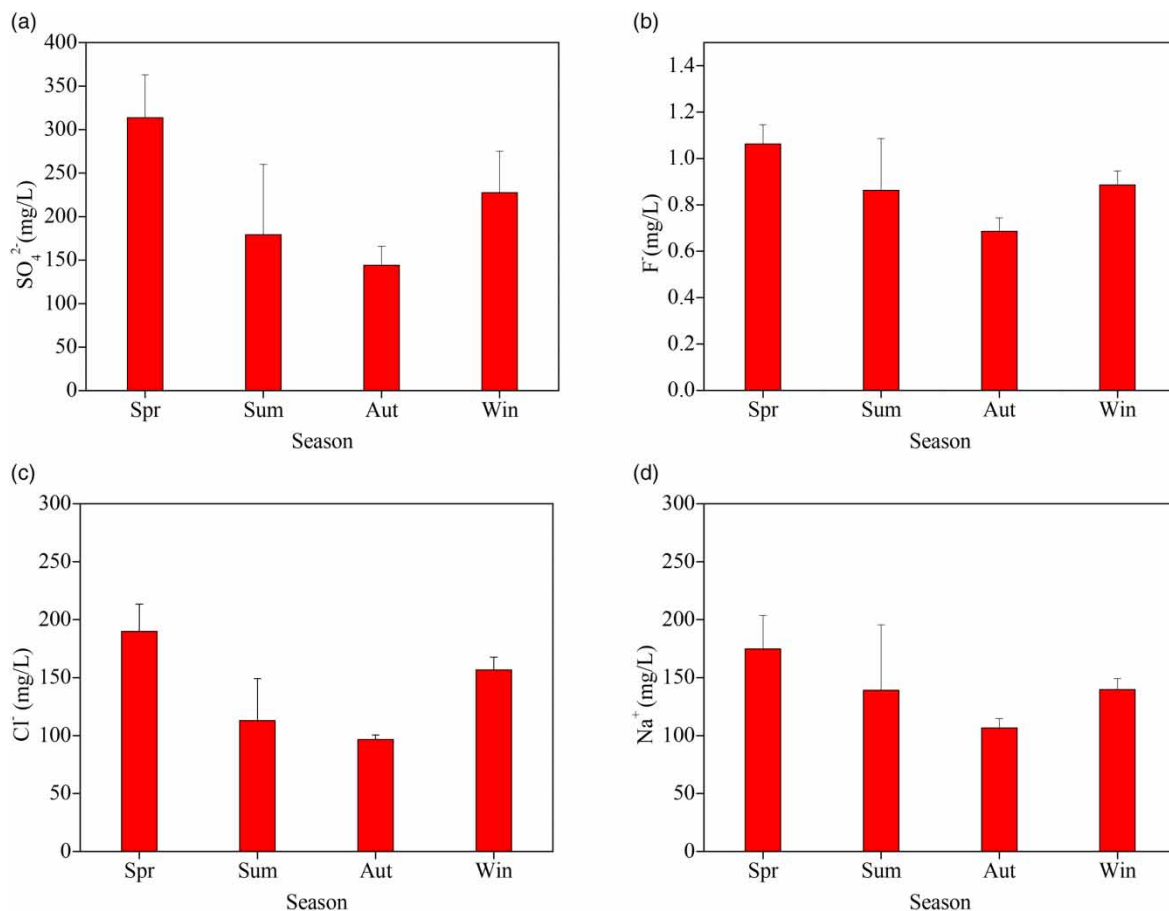


**Figure 4** | Seasonal changes in (a)  $\text{SO}_4^{2-}$ , (b)  $\text{F}^-$ , (c)  $\text{Cl}^-$ , and (d)  $\text{Na}^+$ .

For  $\text{SO}_4^{2-}$ ,  $\text{F}^-$ ,  $\text{Cl}^-$ , and  $\text{Na}^+$  of the four exceeding ions, the maximum value appears in spring. During on-site spring sampling, it can be directly observed that the growth of algae in the Xinbian River is lush, and the water body is slightly red, and the overall water quality is poor (Figure S1). See Supplementary information for detail.

### 3.2.3. Spatial variation in major ions

The changes in  $\text{SO}_4^{2-}$ ,  $\text{F}^-$ ,  $\text{Cl}^-$ , and  $\text{Na}^+$  along the upstream to downstream direction (S1 → S9) are shown in Figure 5. In general, the variation amplitude of  $\text{SO}_4^{2-}$ ,  $\text{F}^-$ ,  $\text{Cl}^-$ , and  $\text{Na}^+$  at each sampling point within the year is small, and no significant difference is observed along the path direction. However, the mean value of the three sampling points (e.g., S7, S8, and S9) after S6 showed an overall decreasing trend.

Notably, among the four over-standard ions of  $\text{SO}_4^{2-}$ ,  $\text{F}^-$ ,  $\text{Cl}^-$ , and  $\text{Na}^+$ , the single sample maximum content of  $\text{SO}_4^{2-}$ ,  $\text{F}^-$ ,  $\text{Cl}^-$ , and  $\text{Na}^+$  all appeared in the S9 sampling point during spring (Suzhou control gate), which may be close to the Liuqiao Gate Bridge, and the water quality is affected by human disturbances, such as hydraulic interception and traffic.

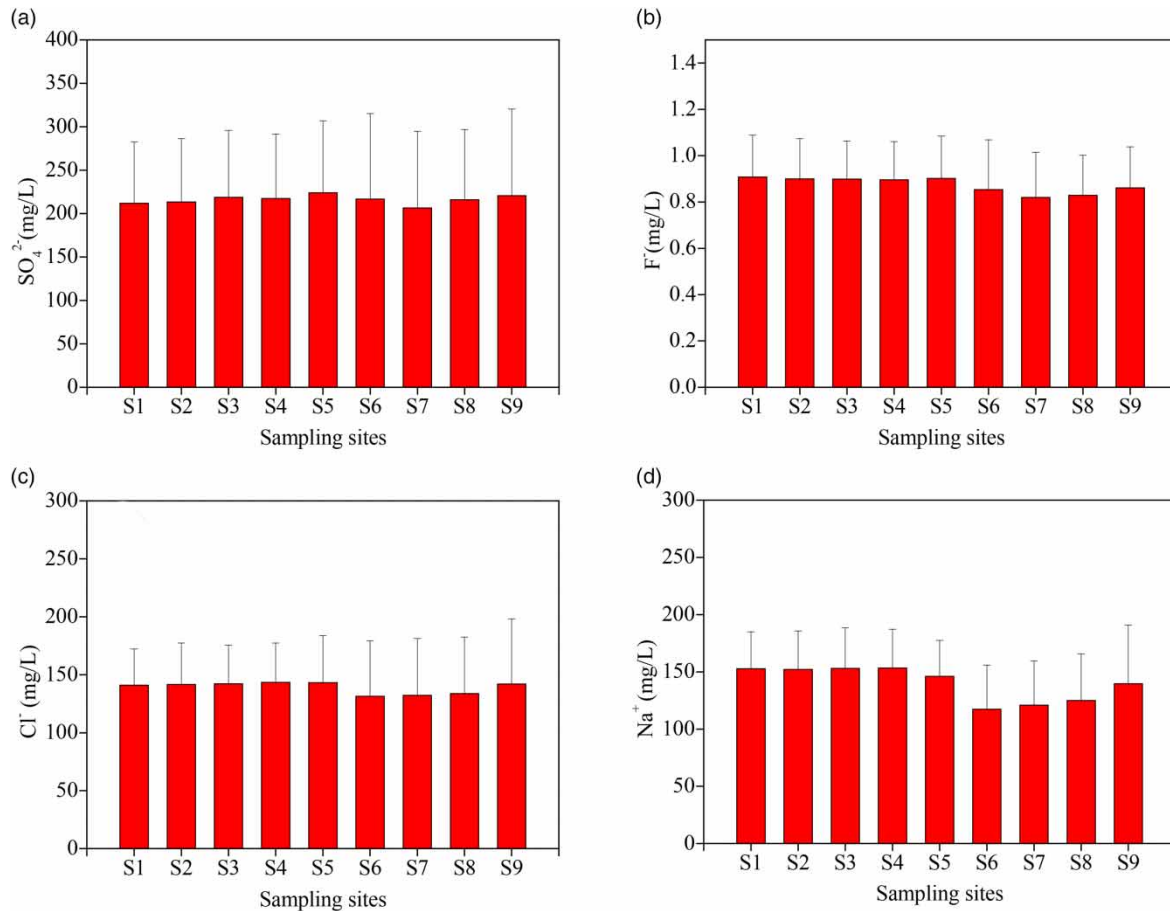


**Figure 5** | Space variation of (a)  $\text{SO}_4^{2-}$ , (b)  $\text{F}^-$ , (c)  $\text{Cl}^-$ , and (d)  $\text{Na}^+$  along the course.

### 3.3. Mechanism of hydrochemical formation

Dividing water chemistry types is of great significance for understanding the hydrological evolution of surface water. A Piper three-line diagram can directly reflect the composition of anion and cation contents in water and is an important means to divide water chemistry types (Piper 1944). Based on the water chemistry software AqQA (version 1.5), the Piper three-line diagram of the samples in spring, summer, autumn, and winter is shown in Figure 6.

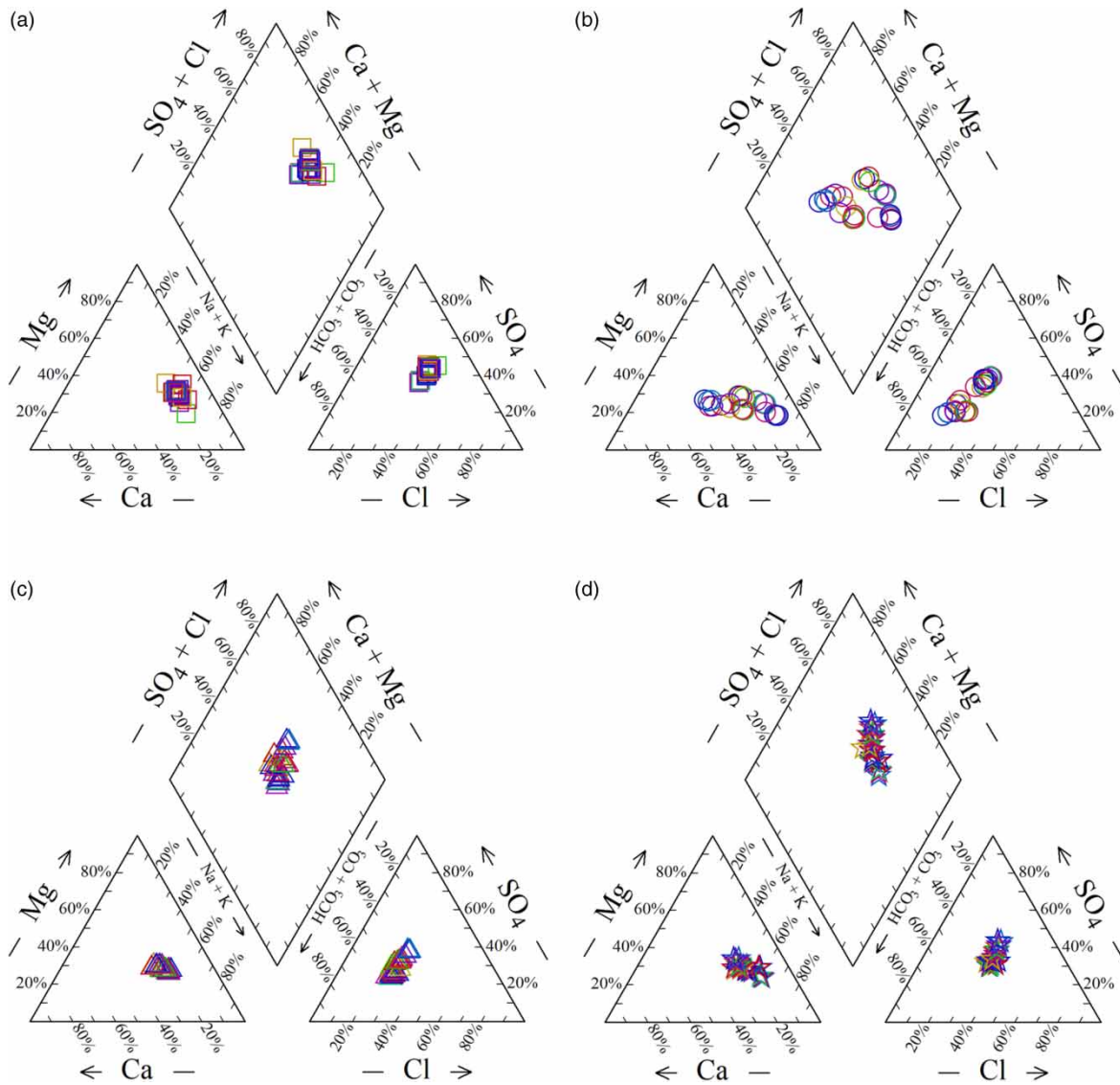
As shown in Figure 6(a), the distribution of samples in 3 months of spring is relatively concentrated. In the cation three-line diagram, most cations in the surface water are dominated by  $\text{Na}^+$ , followed by  $\text{Mg}^{2+}$ . However, in the anionic three-line diagram, the samples are distributed at the position above the middle, thereby showing the dominance of  $\text{SO}_4^{2-}$ . There are 26 Na–Mg– $\text{SO}_4$  type and 1 Na– $\text{SO}_4$  type.

Figure 6(b) displays that the distribution of summer samples in the triline plot is more dispersed than during spring, and the water chemistry type is more complex, which may be related to the intense evaporation and frequent atmospheric rainfall in summer. For this study area, the average annual precipitation and evaporation are 858.1 and 1,589.4 mm, respectively, and the precipitation is mainly concentrated from June to August (Chen *et al.* 2020; Chen *et al.* 2021), and more than 50% of the total precipitation falls from June to September (Lin *et al.* 2017). Overall, most water-like  $\text{Na}^+$  was the dominant cation, whereas  $\text{HCO}_3^-$  was still the main anion, and  $\text{SO}_4^{2-}$  began to be enriched. The hydrochemical types include the following: eight were Na–Ca– $\text{HCO}_3$ , seven were Na–Mg– $\text{SO}_4$ , five were Ca–Na– $\text{HCO}_3$ , four were Na– $\text{SO}_4$ , and three were Na–Mg– $\text{HCO}_3$ .

As shown in Figure 6(c), the distribution of autumn hydrochemical samples in the Piper plot is very concentrated, with  $\text{Na}^+$  dominating, followed by  $\text{Mg}^{2+}$  and  $\text{Ca}^{2+}$ . The anions are mainly  $\text{HCO}_3^-$ , followed by  $\text{SO}_4^{2-}$ . There are 22 Na–Mg– $\text{HCO}_3$  type, 3 Na–Mg– $\text{SO}_4$  type and 2 Na–Ca– $\text{HCO}_3$  type water.

As shown in Figure 6(d), the cations in the river do not change significantly with time, while the dominant anion tends to transition from  $\text{HCO}_3^-$  to  $\text{SO}_4^{2-}$ . In addition,  $\text{Cl}^-$  gradually accumulates. In winter, the chemical types of Xinbian River water included 14 Na–Mg– $\text{SO}_4$  type, 9 Na–Mg– $\text{HCO}_3$  type, and 4 Na–Mg– $\text{Cl}$  type.





**Figure 6** | Piper diagram of water samples in (a) spring, (b) summer, (c) autumn, and (d) winter in the Xinbian River.

Jiang *et al.* (2020) and Chen *et al.* (2020) studied the hydrochemical type of Xinbian River in July 2019 and October 2019 and found that Na–Cl–SO<sub>4</sub> type and Na–HCO<sub>3</sub> type, respectively. Although the obtained hydrochemical types differ from those in this study, the dominant cation (e.g., Na<sup>+</sup>) and anions (e.g., HCO<sub>3</sub><sup>-</sup> and SO<sub>4</sub><sup>2-</sup>) are consistent. The present study further demonstrates that the types of hydrochemicals vary with seasons. Thus, the analysis of hydrochemical control mechanisms in natural water bodies only through a single sampling is not comprehensive.

### 3.4. Water chemical control mechanism

#### 3.4.1. Gibbs graphical method

In the Gibbs figure: rock weathering-dominated samples, evaporation-predominant samples, and atmospheric precipitation-dominated samples are located in the mid-left region, the upper right corner, and the lower right corner of the Gibbs map, respectively (Figure 7).

After calculation, the Gibbs I value of the water samples during spring ranged from 0.53 to 0.69, and the mean value was 0.60; the Gibbs II range was 0.71–0.83, with a mean value of 0.77. The Gibbs I value of the water samples during summer ranged from 0.22 to 0.50, and the mean value was 0.38; the Gibbs II range was 0.44–0.87, with a mean value of 0.69. The Gibbs I value of the water samples during autumn ranged from 0.32 to 0.45, and the average value was 0.38; the Gibbs II range was 0.59–0.72, with a mean value of 0.66. The Gibbs

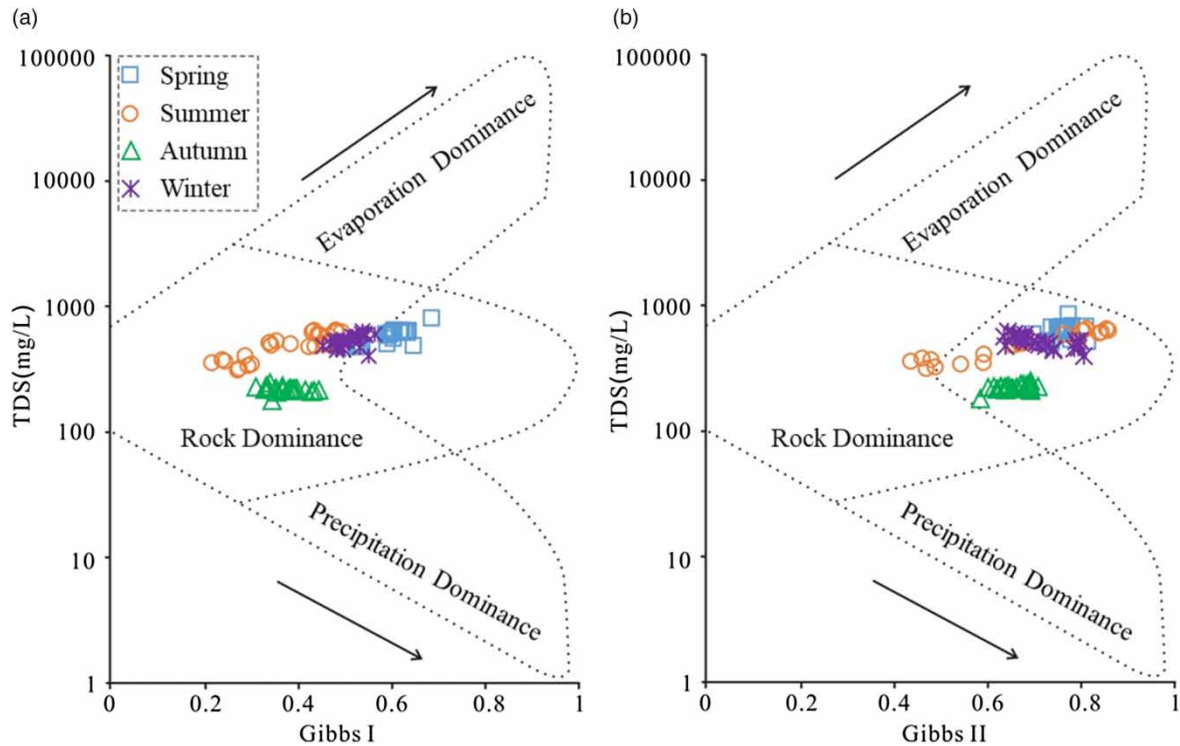


**Figure 7** | Xinbian River water sample Gibbs diagram.

I values of the water samples during winter ranged from 0.46 to 0.57, and the mean value was 0.51; the Gibbs II range was 0.64–0.81, with a mean value of 0.71. From the whole year scale, the Gibbs I range was 0.22–0.69 with a mean value of 0.47 and a Gibbs II range of 0.44–0.87 with a mean value of 0.71.

Figure 7(a) shows that, although the spatial distribution of the samples varies with seasons, they are generally located in the areas dominated by rock weathering, indicating that water–rock interaction is the main controlling factor of the hydrochemical composition of the Xinbian River. However, Figure 7(b) also shows that, the spatial distribution of some samples shifts to the right, indicating that the Xinbian River ion source is not only affected by rock weathering, evaporation crystallization, and atmospheric precipitation, but also has other influencing factors, such as anthropogenic activity and ion exchange (Wang *et al.* 2019).

### 3.4.2. Ion ratio method

$(\text{Mg}^{2+}/\text{Na}^+)/(\text{Ca}^{2+}/\text{Na}^+)$  and  $(\text{HCO}_3^-/\text{Na}^+)/(\text{Ca}^{2+}/\text{Na}^+)$  ion mixing diagrams are effective indicators to qualitatively determine the source of ions in water bodies (Chen *et al.* 2019). The ion ratio method can determine the influence of silicate weathering, evaporite, and carbonate dissolution on the water body by using the molar ratio relationship among different ions. As shown in Figure 8, the sample point is mainly located near the silicate end element, indicating that the solute in the river water is mainly more significantly affected by the weathering of the silicate minerals. Previous studies on the processes controlling river solution of two surface waters (Tuo River and Xinbian River) in the study area through single sampling also had shown that the hydrochemical mechanism of Xinbian River is mainly affected by silicate weathering (Jiang *et al.* 2020). Yu *et al.* (2020a) also found that the hydrochemical formation of shallow groundwater in the study area is mainly affected by the dissolution of silicates.

All the water samples in the Xinbian River in spring, autumn, and winter are located in the area where the silicate is weathered, and the ions in the Xinbian River are mainly affected by the weathering of the silicate rock. From the perspective of the overall distribution of the four seasons, the water sample points tend to deviate from the silicate-weathered zone to the carbonate-weathered zone.

In summer, most of the Xinbian River water sample points are concentrated in the silicate weathering area. At the same time, most sample points have a significant trend of deviation toward the carbonate-weathered zone. Therefore, the ions in the Xinbian River during summer are mainly affected by the weathering of silicate, and

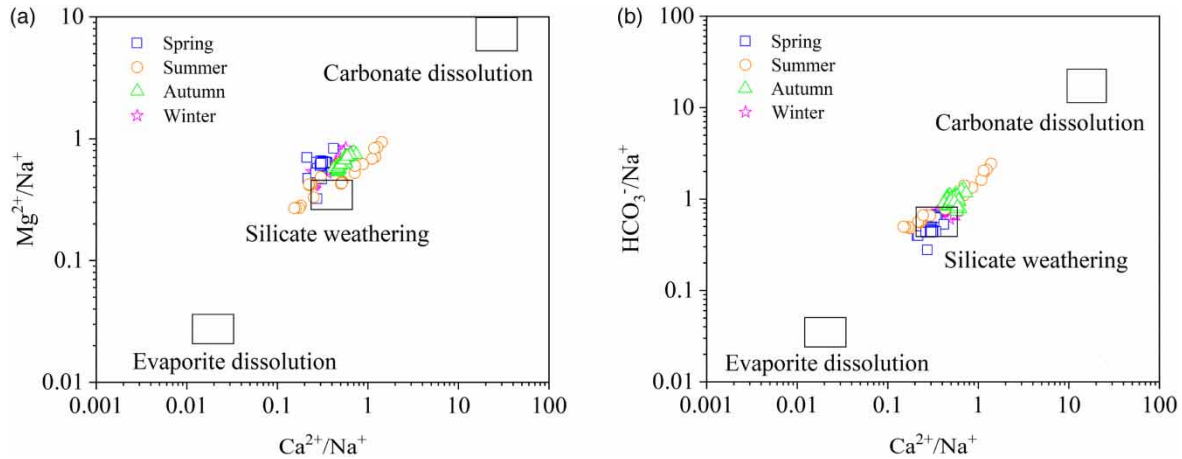


**Figure 8** | Three rock categories. (a)  $(\text{Mg}^{2+}/\text{Na}^+)/(\text{Ca}^{2+}/\text{Na}^+)$  and (b)  $(\text{HCO}_3^-/\text{Na}^+)/(\text{Ca}^{2+}/\text{Na}^+)$ .

a few ions in the water are also affected by the weathering of carbonate. This phenomenon is mainly determined by the climatic and lithological characteristics of the region. Summer rainfall in Suzhou City is sufficient, the temperature is high, and the water flow speed is accelerated, thereby accelerating the water-rock interaction of ions in water. Compared with silicate, which is difficult to weather, carbonates, which are easier to weather are dissolved faster by weathering. Therefore, most sample points in the Xinbian River in summer are biased toward carbonate-weathered areas.

#### 4. CONCLUSIONS

Through a whole year of sampling and testing analysis, this article mainly studied the spatiotemporal changes of physicochemical indicators and routine ions in the nearby city river Xinbian River, in Suzhou City, Anhui Province, China. This article focuses on studying the variation patterns of water quality indicators in different seasons and the mechanism of hydrochemical formation and draws the following main conclusions.

- (1) In the basic physicochemical indexes, pH has no obvious change trend with the season and along the path, and the overall water body is alkaline; DO is increasing with seasonal change and along the process, increasing first and then decreasing, the winter climate condition is more conducive to atmospheric oxygen enrichment, the biological oxygen consumption is small, and the changes along the path may be affected by the control gate.
- (2) In conventional ions,  $\text{SO}_4^{2-}$ ,  $\text{F}^-$ ,  $\text{Cl}^-$ , and  $\text{Na}^+$  tended to decrease first and then increase with the season. The maximum monthly average of excessive ions appears in May, which is likely to be related to the decline in algae, DO, and the overall deterioration of water quality; along the process, the maximum content of  $\text{SO}_4^{2-}$ ,  $\text{Cl}^-$ , and  $\text{Na}^+$  in the single water sample appeared near the control gate and is most likely to be related to human disturbance.
- (3) The water chemistry type of the study reach is dominated by Na-Mg- $\text{SO}_4$  in spring; influenced by strong evaporation and frequent rainfall, mainly Na-Ca- $\text{HCO}_3$  and Na-Mg- $\text{SO}_4$  in summer; Na-Mg- $\text{HCO}_3$  in autumn; and Na-Mg- $\text{SO}_4$  and Na-Mg- $\text{HCO}_3$  in winter. The control factors of water chemical composition somewhat vary with the season, but rock weathering (water-rock interaction) is still the main control factor that is mainly affected by the influence of silicate mineral weathering, especially in spring, autumn, and winter. In summer, a tendency of significant deviation of the silicate toward the carbonate weathering zone is observed and is affected by evaporation crystallization, atmospheric precipitation, human activity, ion exchange, and other factors.

The research results of this article are of great significance for understanding the mechanism of hydrochemical formation and screening the optimal control pollutants in the studied river sections. From the tested indicators in this article, the four indicators including  $\text{SO}_4^{2-}$ ,  $\text{F}^-$ ,  $\text{Cl}^-$ , and  $\text{Na}^+$  should be the focus of monitoring and management. If the Xinbian River was truly used as a source of surface drinking water, it is also necessary to monitor other characteristic pollutants (e.g., heavy metals and organic pollutants, etc.) and carry out source prevention and control of the characteristic pollutants.

## ACKNOWLEDGEMENTS

This research was supported by Anhui Provincial Natural Science Foundation of China (2008085MD122), Open Foundation of State Environmental Protection Key Laboratory of Synergetic Control and Joint Remediation for Soil & Water Pollution (GHBK-2022-001), Natural Resources Science and Technology Project of Anhui Province (2022-k-8), Zhejiang Provincial Natural Science Foundation of China under Grant No. LQ20D010009, Research Development Foundation of Suzhou University (2021fzjj28), and Commonweal geologic work of Anhui Province (2022-g-1-2). We thank Kai Chen, Xiang Zhao, and Linghui Yu very much for their help in sample collection and figure preparation.

## DATA AVAILABILITY STATEMENT

Data cannot be made publicly available; readers should contact the corresponding author for details.

## CONFLICT OF INTEREST

The authors declare there is no conflict.

## REFERENCES

- Chen, Y., Bai, J. W., Yang, J. & Liu, M. Y. 2019 Hydro-geochemistry of surface waters in the northeast slope of Mt. Gongga and its controls. *Journal of Sichuan Agricultural University* **37**(4), 497–503. (In Chinese).
- Chen, K., Sun, L. H. & Tang, J. 2020 Hydrochemical differences between river water and groundwater in Suzhou, Northern Anhui Province, China. *Open Geosciences* **12**(1), 1421–1429.
- Chen, K., Sun, L. H. & Xu, J. Y. 2021 Statistical analyses of groundwater chemistry in the Qingdong coalmine, northern Anhui province, China: Implications for water-rock interaction and water source identification. *Applied Water Science* **11**(2), 50.
- Chen, K., Liu, Q. M., Peng, W. H., Liu, Y. & Wang, Z. T. 2023 Source apportionment of river water pollution in a typical agricultural city of Anhui Province, eastern China using multivariate statistical techniques with APCS– MLR. *Water Science and Engineering* **16**(2), 165–174.
- EPAC (State Environmental Protection Agency of China). & GAQSIQC (General Administration of Quality Supervision, Inspection and Quarantine of China) 2002 *Environmental Quality Standards for Surface Water (GB 3838-2002)*. China Environmental Science Press, Beijing. (in Chinese)
- Gbadebo, A. M. 2020 Assessment of quality and health risk of peri-urban groundwater supply from selected areas of Abeokuta, Ogun State, Southwestern Nigeria. *Environmental Geochemistry and Health* **43**(7), 2743–2755.
- Giri, S. & Singh, A. K. 2014 Risk assessment, statistical source identification and seasonal fluctuation of dissolved metals in the Subarnarekha River, India. *Journal of Hazardous Materials* **265**, 305–314.
- Jiang, Y. Q., Gui, H. R., Yu, H., Wang, M. C., Fang, H. X., Wang, C. L., Chen, C., Zhang, Y. R. & Huang, Y. H. 2020 Hydrochemical characteristics and water quality evaluation of rivers in different regions of cities: A case study of Suzhou City in Northern Anhui Province, China. *Water* **12**(4), 950.
- Jiang, X. Q., Peng, W. H., Yu, L. H., Chen, R., Liu, J. L., Zhao, X. R. & Sun, W. B. 2021a Pollution characteristics and ecological risk of heavy metals in Xinbian River of Suzhou. *Journal of Water Resources Research* **10**(4), 416–425. (In Chinese).
- Jiang, Y. Q., Gui, H. R., Li, C., Chen, J. Y., Chen, C., Wang, C. L., Zhao, H. H., Guo, Y., Xu, J. Y., Li, J. & Qiu, H. L. 2021b Evaluation of the difference in water quality between urban and suburban rivers based on self-organizing map. *Acta Geophysica* **69**, 1855–1864.
- Khan, M. H., Nafees, M., Muhammad, N., Ullah, U., Hussain, R. & Bilal, M. 2021 Assessment of drinking water sources for water quality, human health risks, and pollution sources: A case study of the district Bajaur, Pakistan. *Archives of Environmental Contamination and Toxicology* **80**(1), 41–54.
- Kormoker, T., Idris, A. M., Khan, M. M., Tusher, T. R., Proshad, R., Islam, M. S., Khadka, S., Rahman, S., Kabir, M. H. & Kundu, S. 2022 Spatial distribution, multivariate statistical analysis, and health risk assessment of some parameters controlling drinking water quality at selected primary schools located in the southwestern coastal region of Bangladesh. *Toxin Reviews* **41**(1), 247–260.
- Li, Q. H. 2003 Research and analysis of water pollution of Xin Bian-he River through Suzhou City. *Journal of Suzhou Teachers College* **18**(2), 63–64. (In Chinese).
- Lin, M. L., Gui, H. R., Wang, Y. & Peng, W. H. 2017 Pollution characteristics, source apportionment, and health risk of heavy metals in street dust of Suzhou, China. *Environmental Science and Pollution Research* **24**, 1987–1998.
- Lin, M. L., Yu, H. & Peng, W. H. 2022 Hydrochemical characteristics and irrigation water evaluation of suburban river: A case study of Suzhou City, Anhui Province, China. *Nature Environment and Pollution Technology* **21**(1), 1–10.
- Piper, A. M. 1944 A graphic procedure in the geochemical interpretation of water-analyses. *Eos, Transactions American Geophysical Union* **25**(6), 914–928.
- Prasad, S., Saluja, R., Joshi, V. & Garg, J. K. 2020 Heavy metal pollution in surface water of the Upper Ganga River, India: Human health risk assessment. *Environmental Monitoring and Assessment* **192**(11), 742.

- Qu, J. H. & Fan, M. H. 2010 The current state of water quality and technology development for water pollution control in China. *Critical Reviews in Environmental Science and Technology* **40**(6), 519–560.
- SAMRC (State Administration for Market Regulation of China) & SAC (Standardization Administration of China) 2022 *Standards for Drinking Water Quality (GB 5749-2022)*. China Standard Press, Beijing. (in Chinese)
- Schwarzenbach, R. P., Egli, T., Hofstetter, T. B., Gunten, U. & Wehrli, B. 2010 Global water pollution and human health. *Annual Review of Environment and Resources* **35**(1), 109–136.
- Wang, F. 2020 Research and realization of information management system of Xinbian river water conservancy project. *Shaanxi Water Resources* (5), 143–145. (In Chinese).
- Wang, M. C., Gui, H. R., Hu, R. J., Zhao, H. H., Li, J., Yu, H. & Fang, H. X. 2019 Hydrogeochemical characteristics and water quality evaluation of carboniferous Taiyuan formation limestone water in Sulin mining area in Northern Anhui, China. *International Journal of Environmental Research and Public Health* **16**(14), 2512.
- WHO (World Health Organization) 2017 *Guidelines for Drinking-water Quality*, 4th edn. Incorporating the First Addendum, Geneva.
- Yu, Y. Q. & Feng, S. B. 2018 Distribution characteristics and pollution evaluation of heavy metals in the sediment of Xinbian River in Suzhou. *Western Resources* (3), 123–126. (In Chinese).
- Yu, H., Gui, H. R., Zhao, H. H., Wang, M. C., Li, J., Fang, H. X., Jiang, Y. Q. & Zhang, Y. R. 2020a Hydrochemical characteristics and water quality evaluation of shallow groundwater in Suxian mining area, Huaibei coalfield, China. *International Journal of Coal Science & Technology* **7**(4), 825–835.
- Yu, M. M., Li, Z. C., Li, Q. W., Meng, X. C., Cheng, K. F. & Feng, Y. C. 2020b Evaluation and analysis of water quality in urban rivers of coal cities: A case study of Xinbianhe River in Suzhou City. *Journal of Xichang College (Natural Science Edition)* **34**(2), 55–61. (In Chinese).
- Yu, H., Lin, M. L., Peng, W. H. & He, C. 2022 Seasonal changes of heavy metals and health risk assessment based on Monte Carlo simulation in alternate water sources of the Xinbian River in Suzhou City, Huaibei Plain, China. *Ecotoxicology and Environmental Safety* **236**, 113445.
- Zhang, F., Shi, X. H., Zhao, S. N., Arvola, L., Huotari, J. & Hao, R. N. 2022 Equilibrium simulation and driving factors of dissolved oxygen in a shallow eutrophic Inner Mongolian lake (UL) during open-water period. *Water Supply* **22**(6), 6013–6031.
- Zhou, F. X., Lu, X., Chen, F. J., Zhu, Q. M., Meng, Y. F., Chen, C. Q., Lao, Q. B. & Zhang, S. W. 2020 Spatial-monthly variations and influencing factors of dissolved oxygen in surface water of Zhanjiang bay, China. *Journal of Marine Science and Engineering* **37**(4), 403.

First received 24 October 2023; accepted in revised form 18 February 2024. Available online 4 March 2024